Endocrine (2019) 65:582–594
https://doi.org/10.1007/s12020-019-01910-3

ORIGINAL ARTICLE

Check for updates

miR-650 promotes motility of anaplastic thyroid cancer cells by targeting PPP2CA

Francesca Maria Orlandella[1] · Raffaela Mariarosaria Mariniello[2,3] · Paola Lucia Chiara Iervolino[1] · Esther Imperlini[1] · Annalisa Mandola[2,3] · Anna Verde[2] · Anna Elisa De Stefano[2,3] · Katia Pane[1] · Monica Franzese[1] · Silvia Esposito[2] · Fulvio Basolo[4] · Stefania Orrù[1,3] · Giuliana Salvatore[1,3]

Received: 18 October 2018 / Accepted: 18 March 2019 / Published online: 29 March 2019

Abstract

Purpose Aberrant expression of miRNAs is crucial in several tissues tumorigenesis including thyroid. Recent studies demonstrated that miR-650 plays different role depending on the cancer type. Herein, we investigated the role of miR-650 in thyroid carcinoma.

Methods The expression of miR-650 was analyzed in human thyroid tissues by q-RT-PCR. Anaplastic (8505C, CAL62, SW1736) and papillary (TPC-1) thyroid cancer cell lines were used to dissect the role of miR-650 on malignant hallmarks of transformation. Label-free proteomic analysis was exploited to unravel the targets of miR-650, while luciferase reporter assay and functional experiments were performed to confirm a selected target. Spearman's rank correlation test was used to assess the association between miR-650 and its target in human thyroid cancer tissues.

Results miR-650 is over-expressed in anaplastic (ATC) thyroid carcinoma where it enhances cell migration and invasion. Proteomic label-free and bioinformatics analysis revealed that the serine-threonine protein phosphatase 2 catalytic subunit alpha (PPP2CA) is a target of miR-650; these finding were confirmed by luciferase assay. Restoration of PPP2CA mRNA, deprived of its 3′UTR, is able to revert the malignant phenotype induced by miR-650 in HEK-293 cells. Importantly, PPP2CA is down-regulated in ATC tissues and is inversely correlated with miR-650.

Conclusions miR-650 displayed oncogenic activity in ATC cells through targeting PPP2CA phosphatase. These results suggest that miR-650/PPP2CA axis could be modulated to interfere with motile ability of thyroid carcinoma cells.

Keywords miR-650 · PPP2CA · Thyroid cancer · Motility

Introduction

microRNA (miRNAs) are small non coding RNA that negatively regulate gene expression by pairing the 3′ untranslated region (UTR) of specific target genes [1]. Over-expression of several miRNAs has been involved in distinct step of cancer pathogenesis and in the metastatic process [2, 3]. Indeed, several miRNAs have been classified as oncomiRs being able to down-regulate the expression of specific tumor suppressor genes [4].

In vitro and in vivo evidences demonstrated that miR-650 plays a key role in several human cancers. In fact, its over-expression has been reported in glioma [5], hepatocellular [6], lung [7], breast [8] prostate [9] and gastric cancers. In the latter, over-expression of miR-650 is associated with metastasis [10]. In glioma, in hepatocellular and in lung carcinoma, miR-650 over-expression correlated with high grade of the tumors and poor prognosis. While, in

Supplementary information The online version of this article (https://doi.org/10.1007/s12020-019-01910-3) contains supplementary material, which is available to authorized users.

✉ Giuliana Salvatore
giuliana.salvatore@uniparthenope.it

[1] IRCCS SDN, Napoli, Via Emanuele Gianturco 113, 80143 Napoli, Italy

[2] CEINGE - Biotecnologie Avanzate s.c. a r.l., Via Gaetano Salvatore 486, 80145 Napoli, Italy

[3] Dipartimento di Scienze Motorie e del Benessere, Università "Parthenope", Via Medina 40, 80133 Napoli, Italy

[4] Dipartimento di Patologia Chirugica, Medica, Molecolare e dell' Area Critica dell' Università di Pisa, 56126 Pisa, Italy

chronic lymphocytic leukemia [11] and in colorectal cancer [12], miR-650 over-expression is associated with a favorable prognosis. Therefore, the function of miR-650 seems to be tissue type-dependent. To our knowledge the role of miR-650 in thyroid cancer remains unexplored.

Thyroid cancer derived from follicular cells, includes well differentiated, follicular and papillary thyroid carcinomas (PTC), and undifferentiated or anaplastic thyroid carcinoma (ATC). PTC is characterized by good prognosis; on the contrary, ATC represents the most rare and aggressive variant of thyroid carcinoma, and has poor clinical outcome [13, 14]. Deregulation of miRNAs has been demonstrated to play a key role in the pathogenesis and progression of thyroid carcinoma [15–17].

In the current study, we investigated the role of miR-650 in thyroid carcinogenesis. We demonstrated that miR-650 expression level is higher in ATC respect to PTC and normal thyroids (NT) samples and that miR-650 significantly impairs migration and invasion of ATC cells. Finally, through a label-free proteomic analysis and luciferase assay, we identified protein phosphatase 2 catalytic subunit alpha (PPP2CA) as a direct target of miR-650.

Materials and methods

Tissue samples

For q-RT-PCR studies, thyroid samples include a total of 23 frozen tissues from patients who underwent total or subtotal thyroidectomy at the Department of Surgery of the University of Pisa (Pisa, Italy). In detail, the study group included # 6 normal thyroid (NT), # 12 papillary thyroid carcinoma (PTC) and # 5 anaplastic thyroid carcinoma (ATC) human tissues samples. Normal thyroid tissues were obtained distant from neoplasia or from contralateral thyroid lobe. Informed consent was obtained and the retrospective study was conducted anonymously and it conforms to the principles of the Helsinki Declaration of 1975.

Quantitative real-time PCR (q-RT-PCR)

Total RNA was isolated with mirVana^{TM} miRNA Isolation kit (Thermo Fisher Scientific, Waltham, USA) according to the manufacturer's instructions and quantified using the NanoDrop spectrophotometer (Thermo Fisher Scientific, Waltham, USA).

For miRNA detection, 10 ng of total RNA from each sample was reverted in cDNA using a miRNA Reverse Transcription Kit (Thermo Fisher Scientific, Waltham, USA).

For mRNA expression analysis, 1 µg was reversed with the QuantiTect® Reverse Transcription (Qiagen, Crawley, UK) according to manufacturer's instructions.

The expression levels of miR-650 and PPP2CA were measured by q-RT-PCR using specific primers and TaqMan Universal PCR Master Mix (Thermo Fisher Scientific, Waltham, USA). β-ACTIN and U6 snRNA were used as endogenous controls for mRNA and miRNA, respectively.

PCR reactions were performed four times in triplicate and fold changes were calculated by $2^{-\Delta\Delta CT}$ methods.

miR-650 expression from Gene Expression omnibus (GEO) database

Microarray data were downloaded from the National Center for Biotechnology Information (NCBI) GEO database (accession number GSE73182) using R version 3.5.2. Dot plot shows the Log2 transformed expression value of miR- after the full quantile normalization for GEO dataset.

Cell cultures

Papillary thyroid cancer cell line (TPC-1) and anaplastic thyroid cancer cell lines (CAL62, SW1736, 8505C) were maintained in culture in Dulbecco's Modified Eagle Medium (DMEM) containing 10% of fetal bovine serum (FBS), L-glutamine and penicillin/streptomycin (Thermo Fisher Scientific, Waltham, USA).

All the cell lines were authenticated by short-tandem repeat profiling performed by BMR Genomics (http://www.bmr-genomics.it) (Padova, Italy).

Plasmids

miR-650 precursor (HmiR0363-MR04) and negative control (CmiR0001-MR04, named miR-Null); as well as miR-650 inhibitor (HmiR-AN0760-AM01, named Anti miR-650) and negative control (CmiR-AN0001-AM01, named Anti miR-Null); PPP2CA (EX-C0306-M43) plasmids were obtained from GeneCopoeia (Rockville, MD, USA).

Transfection

For stable cells generation, CAL62, 8505C and TPC-1 cells (1×10^5) were transfected using Lipofectamine 2000 (Thermo Fisher Scientific, Waltham, USA) and 4 µg of plasmids according to manufacturer's protocol. Cell clones and mass populations were selected with Puromycin (Sigma-Aldrich, St. Louis, MO, USA) and analyzed for miR-650 expression by q-RT-PCR. One mass population for each cell line was selected and used in all experiments.

For transient cell transfection of SW1736 cells, 4×10^5 cells were transfected with 2 µg of Anti miR-650 and with

its corresponding control (Anti miR-Null) plasmids by using Lipofectamine 2000 (Thermo Fisher Scientific, Waltham, USA) in 6-well plates. Twenty-four hours after transfection, migration and invasion assays, were performed. Transient transfection efficiency was verified by q-RT-PCR.

For transient cell transfection of HEK-293 cells, 2×10^4 cells were incubated with 2 µg of PPP2CA plasmid or with 2 µg of miR-650 plasmid or co-transfected with 1 µg of each plasmid. Untransfected HEK-293 cells were used as a control.

Cell proliferation

For cell proliferation curves, 8505C and CAL62 were plated at a concentration of 3×10^4 cells/well in 6-well plates and counted, in triplicate, at 24, 48, 72 and 96 h.

To determine cell viability MTS assay (tetrazolium compound [3-(4,5-dimethyl-2-yl)-5-(3-carboxymethoxyphenyl)-2-(4-sulfophenyl)-2H-tetrazolium, inner salt) was performed. To this aim, 1×10^3 cells were plated in multi-wells, in triplicate and after 72 and 96 h the CellTiter 96® AQueous One Solution Cell Proliferation Assay (Promega, Madison, WI, USA) was used according to manufacturer. Experiments were repeated three times in triplicates.

Migration assay

To perform wound healing assays, 8505C, TPC-1, CAL62 and SW1736 transfected cells were plated in 6-well plates. A scratch was generated with a micropipette tip on a monolayer of confluent cells and images were taken immediately and after the wound closure. Distances in the wound areas were measured using the Cell[a] software (Olympus, Tokyo, Japan) and expressed as percentage of wound closure. Experiments were repeated three times in triplicates.

For Transwell migration assay, 1×10^5 cells were plated onto the upper well of membrane filter of 8 µm pore size (Costar, Cambridge, MA, USA). Cells were allowed to migrate for 24 (8505C) or for 48 (CAL62) hours. Migrated cells were stained with crystal violet and quantified at optical density (O.D.) 550 nm.

For Collagen I migration assay, 1.5×10^5 cells were plated on a membrane coated with Collagen I at the bottom side using the CytoSelect™ 24-Well Cell Haptotaxis Assay (Cell Biolabs Inc, San Diego, CA, USA) according to manufacturer.

Invasion assay

For Matrigel Matrix invasion assay, cells (1×10^5) were resuspended in DMEM 5% FBS and plated on the upper chamber of a transwell coated with Matrigel (BD Biosciences, San Jose, CA). DMEM containing 10% FBS was used in the lower chamber as attractant. After 24 (8505C, TPC-1) or 48 (CAL62, SW1736) hours, the invading cells were fixed with glutaraldehyde (11%) (Sigma-Aldrich, St. Louis, MO, USA) for 90 min, stained with crystal violet and quantified at O.D. 550 nm. Experiments were repeated three times.

Invasion in Collagen I Matrix was performed using CytoSelect™ 24-Well Cell Invasion assay (Cell Biolabs Inc, San Diego, CA, USA). Briefly 2×10^5 cells were plated in each well, and allowed to migrate for 24 (8505C) or 48 (CAL62) hours. Invaded cells in Collagen I were measured according to manufacturer's protocol.

Soft agar colony formation assay

Briefly, DMEM containing noble agar (0.5%) was added to Petri dishes (60 mm) and allowed to solidify at room temperature for 30 minutes. Next, 8×10^4 cells were resuspended in DMEM containing noble agar and plated onto the solidified agar Petri dish. Cells were periodically observed under a microscope to monitor colonies formation. After 3 weeks, colonies were photographed and counted with an optical microscope at ×10 magnification. Experiments were repeated two times in triplicates.

Label-free proteomic analysis

CAL62 cells were lysed in a modified RIPA buffer (150 mM NaCl, 50 mM Tris-HCl pH 7.5, 1 mM EDTA, 1% Triton X-100, protease inhibitors). Cell debris was removed by centrifugation and protein concentration was determined using Bradford assay [18]. Protein extract was resuspended in Laemmli buffer and separated on 10% polyacrylamide SDS-PAGE as previously described [19].

Protein bands were manually cut. Gel particles were washed as previously described [20] and then digested with 10 ng/µl modified porcine trypsin (sequencing grade; Promega, Madison, WI).

Peptide mixtures were analyzed by LTQ-Orbitrap XL (Thermo Fisher Scientific, Waltham, USA) and separated on a capillary chromatographic system consisting of a 2 cm length trapping column (C18, ID 100 µm, 5 µm) and a 20 cm C18 reverse phase silica capillary column (ID 75 µm, 5 µm) (Nanoseparations, Nieuwkoop, Netherlands).

Peptides were fragmented in acetonitrile based eluents (Solvent A: 0.2% formic acid, 2% acetonitrile in water; Solvent B: 0.2% formic acid, 5% water in acetonitrile with a gradient from 10 to 40% of B in 80 min, and then from 40 to 95% in 10 min, at 0.25 µL/min flow rate) by using CID fragmentation in the ion trap.

Peptide analysis was performed using data-dependent acquisition of MS scan (400-1,800 m/z) followed by MS/MS scans of the five most abundant ions.

Raw data in.mgf format were processed by Proteome Discoverer platform version 1.4 (Thermo Fisher Scientific, Waltham, USA) interfaced with an in-house Mascot server. Proteins were identified with the following search parameters: UniProt as database, limited to *Homo sapiens* taxonomy; trypsin as a specific proteolytic enzyme; allow up to 1 missed cleavages; 10 ppm precursor tolerance and 0.6 Da fragment ion tolerance; carbamidomethylation of cysteine as a fixed modification; N-terminal glutamine conversion to pyro-glutammic acid and oxidation of methionine as a variable modifications. Only the proteins with at least 2 assigned peptides with an individual MASCOT score > 19 were considered significant.

For label-free analysis, spectral counts were used for estimating protein abundance and comparing the expression of the same protein between the two cell lines as previously described [21].

The differentially expressed proteins were analyzed by STRING (https://string-db.org/) in order to classify proteins according to gene ontology (GO) terms and to obtain a protein interaction network [21, 22].

Western blot

Protein extractions and Western blots were conducted according to standard protocol. The following antibodies were used: anti-PPP2CA (Cat # 05-421, Merck-Millipore, Darmstadt, Germany) diluted 1:500; anti-α TUBULIN (Cat # T 9026, Sigma-Aldrich, St. Louis, MO, USA) diluted 1:10000; anti-mouse secondary antibody (Bio-Rad, Hercules, USA) diluted 1:3000. Antigen-antibody complexes were visualized using the chemiluminescence detection solution (Thermo Fisher Scientific, Waltham, USA) and analyzed on a Bio-Rad Chemidoc (Bio-Rad, Hercules, USA). Band intensities were quantified densitometrically relative to the α TUBULIN band (used as endogenous control) using the Molecular Imager ChemiDoc XRS (Bio-Rad, Hercules, USA). Quantification of band intensities was performed with the Image Lab™ software version 6.0 (Bio-Rad, Hercules, USA).

Luciferase reporter assay

The 3′UTR of human PPP2CA (LightSwitch™, PPP2CA_3′UTR/S808927) containing the putative miR-650 binding site, as well as the 3′UTR of control vector (ACTB_3′UTR/S805753) and of the reporter vector (EMPTY_3′UTR/S890005) were purchased from SwitchGear Genomics (La Hulpe, Belgium).

Deletion in the potential miR-650 binding site of the 3′UTR of PPP2CA was introduced by using the QuikChange Site-Directed mutagenesis kit (Agilent Technologies, Santa Clara, USA) and the following oligonucleotides: Forward primer: 5′-gtgccatataaaaatacaaagcttgtcatcaacagccgtg-3′; Reverse primer: 5′-cacggctgttgatgacaagctttgtatttttatatggcac-3′.

The, 8505C/miR-650 and 8505C/miR-Null cells were seeded into a 96-well plate (1×10^3 cells per well) and transfected with the above listed plasmids using FuGENE Transfection Reagent (Roche, Basel, Switzerland) according to standard protocols.

Cells were harvested 24 h post transfection and luciferase activity was measured using the LightSwitch™ Luciferase Assay reagent (SwitchGear Genomics, La Hulpe, Belgium) according to the manufacturer's protocol. Experiments were repeated three times in triplicates.

Statistical analysis

Unpaired t test, used for all statistical analysis, was done with GraphPad Prism 6 software (La Jolla, CA, USA). Data are reported as the mean of replicates experiments done in triplicate ± standard deviation (SD) values. Differences were considered significant when $p < 0.05$. The correlation between miR-650 and PPP2CA expression levels in thyroid tissues was calculated using Spearman's rank correlation test.

Results

miR-650 is over-expressed in human anaplastic thyroid carcinoma samples

We evaluated miR-650 expression by q-RT-PCR in 6 NT, 12 PTC and 5 ATC human tissues samples. Figure 1a shows that miR-650 was significantly over-expressed ($p = 0.0299$) in ATC respect to NT samples. PTC samples showed variable expression of miR-650; not statistically

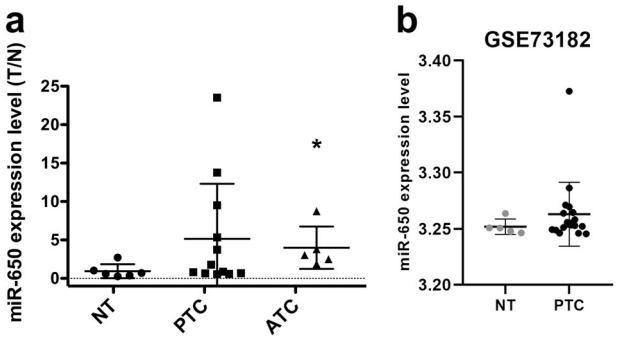

Fig. 1 Expression level of miR-650 in thyroid tissue samples. **a** The level of miR-650 in NT ($n = 6$), PTC ($n = 12$) and ATC ($n = 5$) was determined by q-RT-PCR, performed four times in triplicate. The fluorescence threshold of PTC and ATC samples was compared with the average fluorescence threshold of NT samples. **b** Dot plot of miR-650 expression level in NT ($n = 5$) and PTC ($n = 19$) samples from GSE73182. *$p < 0.05$

significant difference ($p = 0.1760$) was seen compared to NT tissues. Clinicopathological features of PTC patients are listed in Supplementary Table 1. Additionally miRNA expression profiles of 19 PTC and 5 NT extracted from microarray dataset GSE73182 [23], showed no statistical significant difference of miR-650 between NT and PTC ($p = 0.2$) (Fig. 1b).

Forced expression of miR-650 increased cell migration in 8505C cells

To investigate the relevance of miR-650 in anaplastic thyroid cancer progression we selected the thyroid cancer cell line, 8505C for stable transfection with miR-650 plasmid or with a control vector (miR-Null). A mass population expressing the highest level of miR-650 was chosen by q-RT-PCR for further experiments (Supplementary Fig. 1a).

We initially investigated the role of miR-650 in ATC cell migration by wound closure assay. As shown in Fig. 2a, miR-650 significantly increased the capability of 8505C cells to migrate into the wound respect to 8505C/ miR-Null cells. Accordingly, forced expression of miR-650 in 8505C cells, increased the number of migrated cells in the Transwell (Fig. 2b).

To better characterize the migratory properties induced by miR-650 in our cell model system, we plated 8505C/miR-

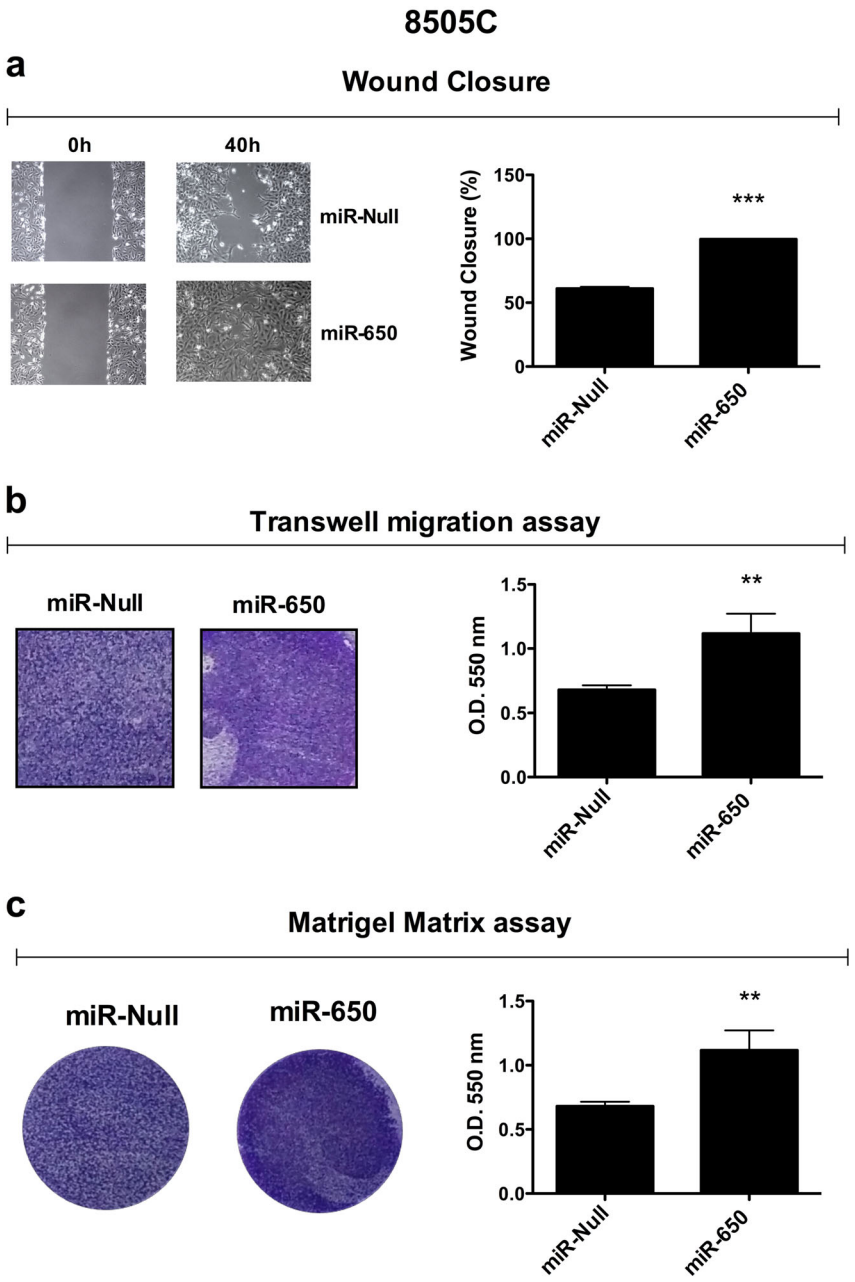

Fig. 2 Role of miR-650 forced expression on cell motility. **a** The wound gaps of 8505C cells stably transfected with miR-650 and with miR-Null plasmids were photographed (left) and measured (right) at 0 and 40 h time points. **b** 8505C/ miR-650 and 8505C/miR-Null cells were plated and allowed to migrate in the Transwell for 24 h; migrated cells were photographed (left) and quantified (right) measuring the absorbance at O.D. 550 nm. **c** 8505C/miR-650 and 8505C/ miR-Null cells were plated on Matrigel Matrix and allowed to invade for 24 h. Cells were then stained and photographed. Invasion ability is expressed as absorbance at O.D. 550 nm. $^{**}p < 0.01$; $^{***}p < 0.001$

650 and 8505C/miR-Null on the bottom side of an insert coated with Collagen I Matrix. After 24 h, 8505C/miR-650 presented an increased ability to migrate into Collagen I compared with 8505C/miR-Null cells (Supplementary Fig. 1b).

Forced expression of miR-650 increased cell invasion in 8505C cells

Then, we studied the effects of miR-650 on cellular invasion by Matrigel Matrix assay. 8505C/miR-650 and 8505C/miR-Null cells were plated on Matrigel and allowed to invade for 24 h. Invasive cells were stained, photographed and quantified at O.D. 550 nm. As shown in Fig. 2c, 8505C/miR-650 are able to degrade the Matrigel layer at higher-level respect to 8505C/miR-Null cells.

Likewise, we also evaluated cell invasion in Collagen I Matrix. As shown in Supplementary Fig. 1c, miR-650 increased the ability of 8505C cells to invade the Collagen I compared to 8505C/miR-Null cells.

Finally, we evaluated cell proliferation in transfected cells by counting cell number and by MTS assay. As shown respectively, in Supplementary Fig. 1d and 1e, the restoration of miR-650 did not affect proliferation rate in 8505C cells.

Forced expression of miR-650 increased cell migration and invasion in TPC-1 cells

The above-described results were also confirmed in another cell line, TPC-1 derived from papillary thyroid carcinoma. TPC-1 cells were stably transfected with miR-650 and with miR-Null plasmids. After selection in Puromycin, cell clones and mass populations were isolated. On the basis of miR-650 expression by q-RT-PCR, one mass population and the respective control was chosen (Fig. 3a) to analyze the biological effects. As shown in Fig. 3b TPC/miR-650 cells have an increased migration rate compared to control miR-Null cells. Likewise, miR-650 forced expression in TPC-1 cells was associated with increased invasion capability (Fig. 3c).

Silencing of miR-650 reduced cell migration and invasion in ATC cells

We next investigated whether stable silencing of miR-650 is able to revert the ATC phenotype. To this aim, we have chosen CAL62, expressing endogenous level of miR-650, for stable transfection with Anti miR-650 or with control vector (Anti miR-Null) plasmids. In Supplementary Fig. 2a, is shown, by q-RT-PCR, that a selected mass population presented reduced level (~2-fold) of miR-650 compared to control cells.

To assess the role of miR-650 on migration ability of CAL62 cells, we performed a wound closure assay. As shown in Fig. 4a, silencing of miR-650 led to a significant reduction of the ability of CAL62 cells to repair the wound respect to CAL62/Anti miR-Null cells. Similar results were obtained when we plated CAL62/Anti miR-650 and control cells on Transwells (Fig. 4b) or on Transwell insert coated with Collagen I (Supplementary Fig. 2b).

Furthermore, CAL62/Anti miR-650 displayed lower invasion ability in Matrigel (Fig. 4c) and in Collagen I Matrix (Supplementary Fig. 2c) compared to control cells.

Finally, to characterize the capability of CAL62/Anti miR-650 cells to growth in an anchorage-independent manner, we performed a soft agar colony formation assay. Strikingly, as shown in Fig. 4d silencing of miR-650 caused an inhibition of colony formation respect to control cells.

Additionally, we confirmed these results in another ATC cell line, SW1736. After transient transfection of Anti miR-650 and control plasmids (Fig. 5a), we observed a significant reduction of wound healing closure (Fig. 5b) and of the number of invading cells (Fig. 5c) in SW1736/Anti miR-650 respect to SW1736/Anti miR-Null transfected cells.

Identification of miR-650 targets by label-free proteomic analysis

To unveil targets of miR-650, we analyzed the protein expression profiles of CAL62/Anti miR-650 compared to CAL62/Anti miR-Null cells. Label-free proteomic analysis based on spectral counting was used to quantitatively compare the protein expression profiles in the two conditions. In particular, it has been calculated the semi-quantitative parameter Rsc, representing the log2 ratio between the protein expression level of CAL62/Anti miR-650 versus Anti miR-Null cells.

This label-free method revealed 351 differentially expressed proteins with Rsc ≥ 2.50 or ≤−2.50. A full list of identified proteins is summarized in Supplementary Table 2. In Supplementary Table 2 such protein species are ranked from the highest Rsc value to the lowest, thus showing 159 over-expressed and 192 under-expressed proteins.

Afterwards we analyzed the 351 deregulated proteins by using STRING software in order to unravel relevant biological pathways and networks among the identified proteins; the top-ranked KEGG pathways are shown in Supplementary Table 3. The network distribution of under-expressed (Supplementary Fig. 3a) and over-expressed (Supplementary Fig. 3b) proteins reveals several protein nodes such as serine/threonine-protein phosphatase 2 A catalytic subunit alpha isoform (PPP2CA), listed among the top-four over-expressed proteins in Supplementary Table 2.

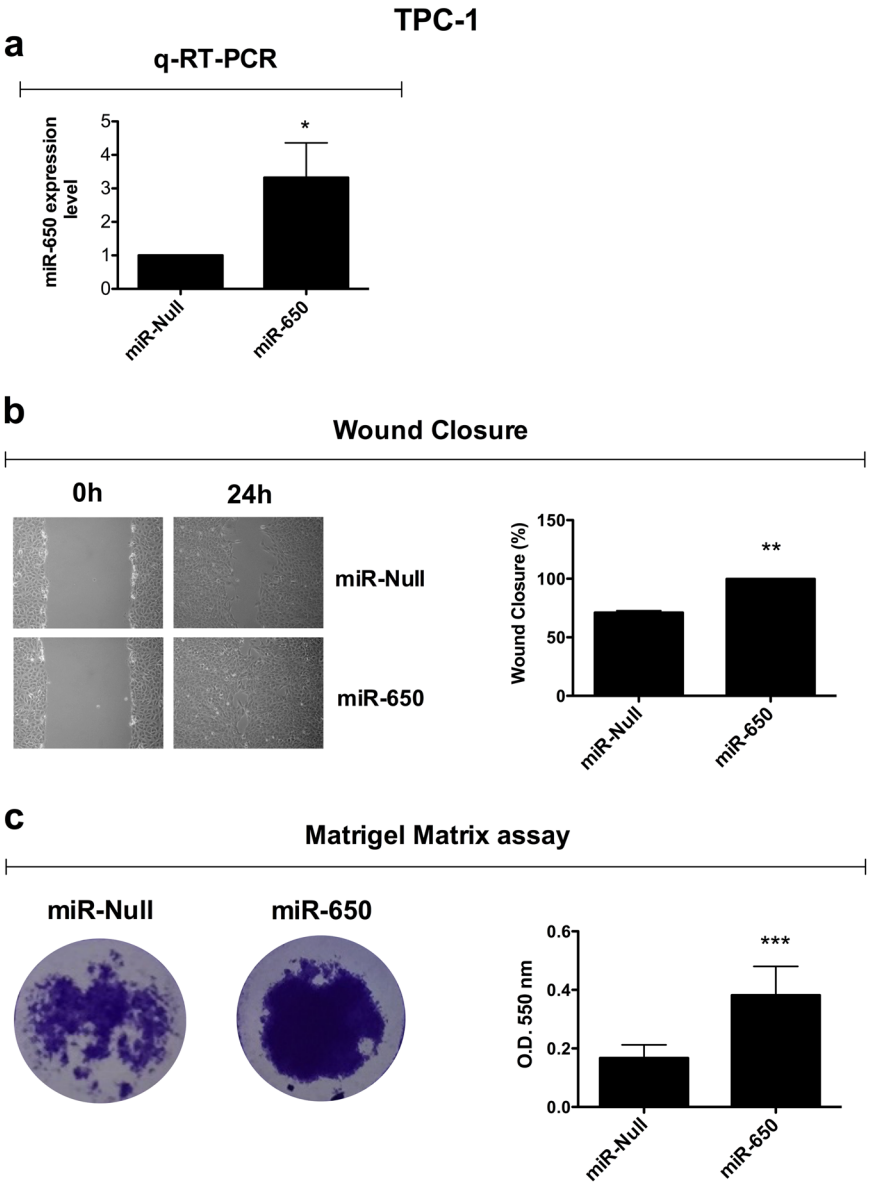

Fig. 3 Role of miR-650 forced expression in TPC-1 cell line. **a** Expression level of miR-650 by q-RT-PCR in TPC-1 mass population cells stably transfected with miR-650 and with miR-Null plasmids. **b** Wound scratches were generated in TPC-1 transfected cells, closures were monitored and photographed. **c** TPC/miR-650 and TPC/miR-Null cells were plated on Matrigel Matrix and cells were allowed to invade for 24 h. $*p < 0.05$; $**p < 0.01$; $***p < 0.001$

PPP2CA is a direct target of miR-650 in ATC cell lines

In support to proteomic data, several bioinformatics algorithms (PITA, MicroT4, RNAhybrid) showed that human PPP2CA mRNA is a predicted miR-650 target, displaying a specific seed sequence in its 3'UTR region for the binding of this miRNA (Fig. 6a).

Then, we measured the expression level of PPP2CA in the cell system in which we performed the proteomic label-free analysis. As illustrated in Fig. 6b (by q-RT-PCR) and in Fig. 6c (by Western blot), PPP2CA mRNA and protein levels were increased in CAL62/Anti miR-650 compared to CAL62/Anti miR-Null cells.

In addition, we determined the expression of PPP2CA also in 8505C/miR-650 cells in which we have performed previous experiments. We found that forced expression of miR-650 inhibited PPP2CA expression at mRNA (Fig. 6d) and at protein (Fig. 6e) levels in 8505C cells compared to control.

Given these results, we next determined whether PPP2CA is a direct target of miR-650 in ATC cells by luciferase assay. Thus, we transfected the 3′UTR of PPP2CA wild type and its deleted form (reported in Fig. 6a) cloned downstream luciferase in 8505C/miR-650 and in 8505C/miR-Null cells. Upon transfection of 3′UTR of PPP2CA wild type, luciferase activity significantly decreased in 8505C/miR-650 cells compared to control (Fig. 6f) conversely, the luciferase activity was unaffected, when a miR-650 binding site in the 3-UTR of PPP2CA was deleted (Fig. 6d). The data indicates that PPP2CA is a direct target of miR-650.

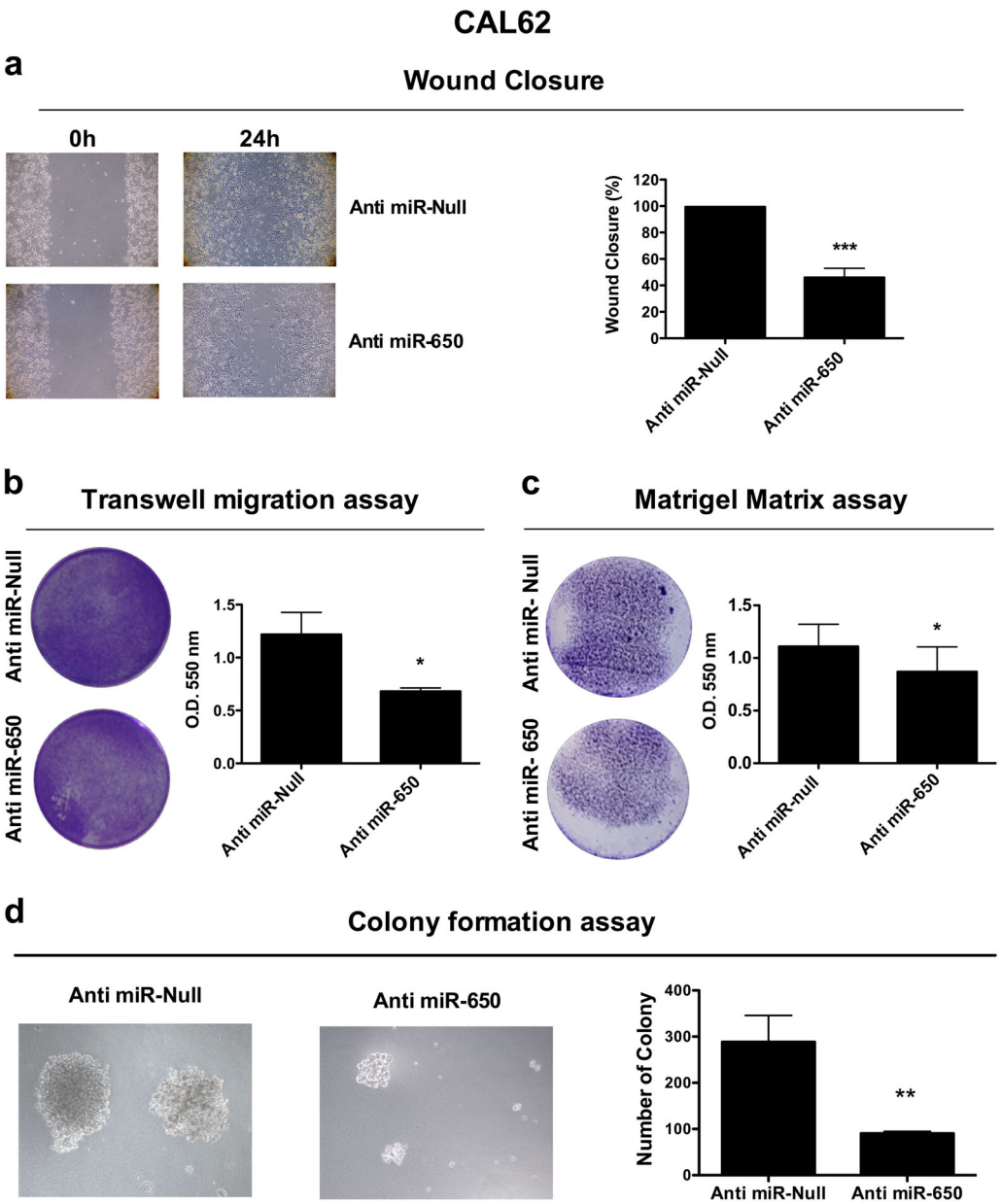

Fig. 4 Effects of miR-650 silencing in CAL62 cell line. **a** The wound gaps of CAL62/Anti miR-650 and control cells were photographed (left) and measured (right) at 0 and 24 h time points. **b** CAL62/Anti miR-650 and CAL62/Anti miR-Null cells were plated and allowed to migrate for 48 h in a Transwell insert. Migration ability is expressed as absorbance at O.D. 550 nm. **c** CAL62/Anti miR-650 and CAL62/Anti miR-Null cells were plated onto the Matrigel Matrix, after 48 h invading cells were photographed (left) and quantified (right) at O.D. 550 nm. **d** CAL62/Anti miR-650 and Anti miR-Null cells were plated in soft agar and photographed after 3 weeks. The number of colonies formed in semisolid medium was counted. $*p < 0.05$; $**p < 0.01$; $***p < 0.001$

PPP2CA rescue the migratory phenotype induced by miR-650

In order to verify if PPP2CA is also a functional target of miR-650, we performed a rescue experiment in an independent human cell line HEK-293. To this aim, we transiently transfected HEK-293 cells with miR-650 or with PPP2CA or with both plasmids and we evaluated the capability of these cells to migrate in a Transwell insert in comparison to untransfected cells. Importantly, the plasmid encodes for an mRNA of PPP2CA deprived of its 3′UTR so that miR-650 is not able to bind.

As shown in Fig. 7a, HEK-293 transfected with miR-650 alone had strong ability to migrate into the Transwell insert, while HEK-293 transfected with PPP2CA abates miR-650

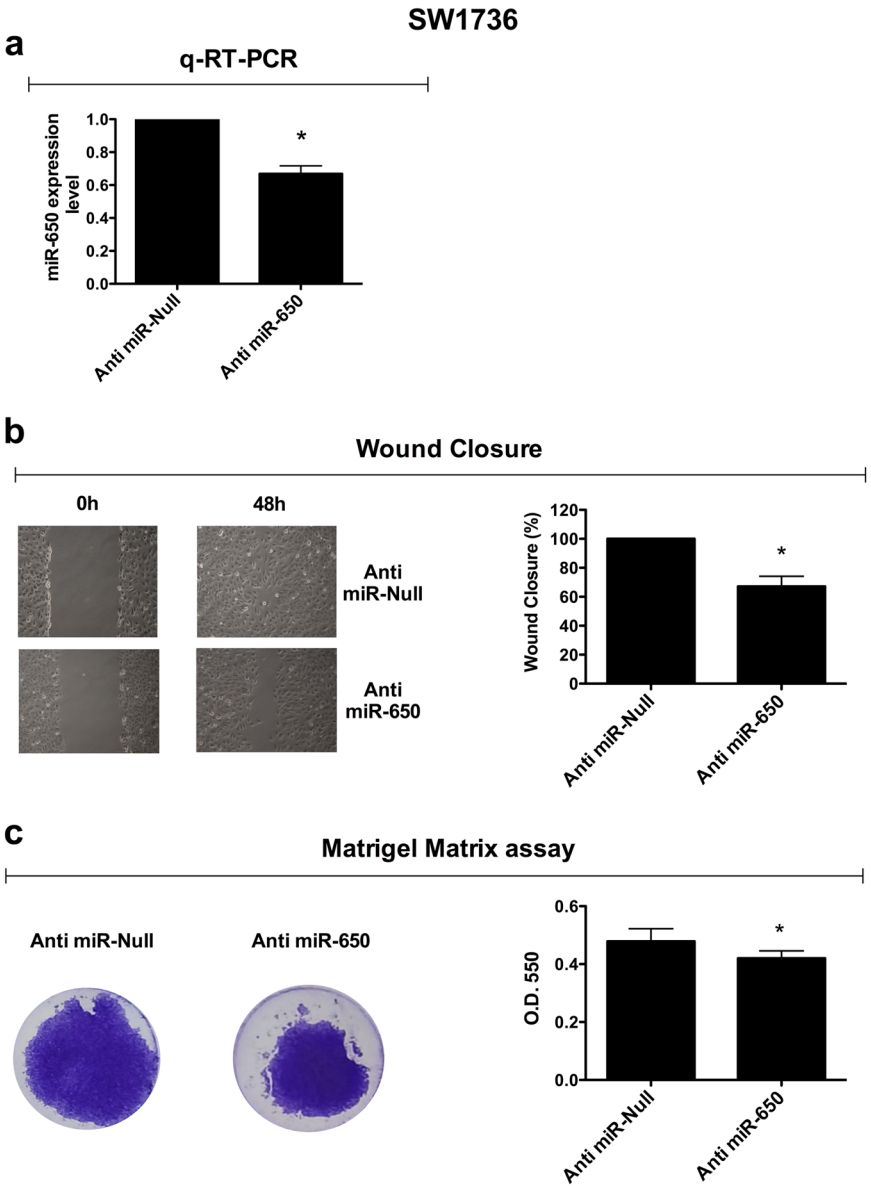

Fig. 5 Effects of miR-650 silencing in SW1736 cell line. **a** Anti miR-650 and Anti miR-Null plasmids were transiently transfected in SW1736 cells and, after 72 h, transfection efficiency was evaluated by q-RT-PCR. **b** Twenty-four hours post transient transfection, a scraped wound was introduced, and cell migration into the wound was photographed (left) and measured (right) at 0 and 48 h time points. **c** Cells, transfected with Anti miR-650 and Anti miR-Null plasmids, were plated onto the Matrigel Matrix transwells and incubated for 48 h. Invading cells were photographed (left) and quantified (right) at O.D. 550 nm. *$p < 0.05$

effects on cell migration, demonstrating that PPP2CA is a functional target of miR-650.

PPP2CA mRNA is reduced in ATC tissues and is inversely correlated with miR-650

Finally, to evaluate the relationship between miR-650 and PPP2CA, we analyzed the expression of PPP2CA mRNA in the same dataset in which we have previously analyzed miR-650 level. As shown in Fig. 7b, q-RT-PCR revealed that PPP2CA is down-regulated in ATC respect to PTC and NT samples. Likewise, we found a significant inverse correlation between miR-650 expression and PPP2CA mRNA ($R = -0.5191$, $p = 0.027$) (Fig. 7c). These results demonstrated that PPP2CA is an in vivo target of miR-650.

Discussion

miRNAs are post-transcriptional regulators involved in a broad spectrum of cellular process, including proliferation, migration and metastasis [1]. Aberrant expression of miRNAs plays an important role in initiation and progression of thyroid cancer [15].

Recently, among altered miRNAs, miR-650 has emerged to play a critical role in the development and progression of many types of tumors [24]; nevertheless its involvement in thyroid carcinogenesis needs to be elucidated.

Here we showed that miR-650 is over-expressed in ATC samples, however, one limitation of this study is the low number of ATC analyzed, this is due to the rarity of this aggressive form of thyroid cancer.

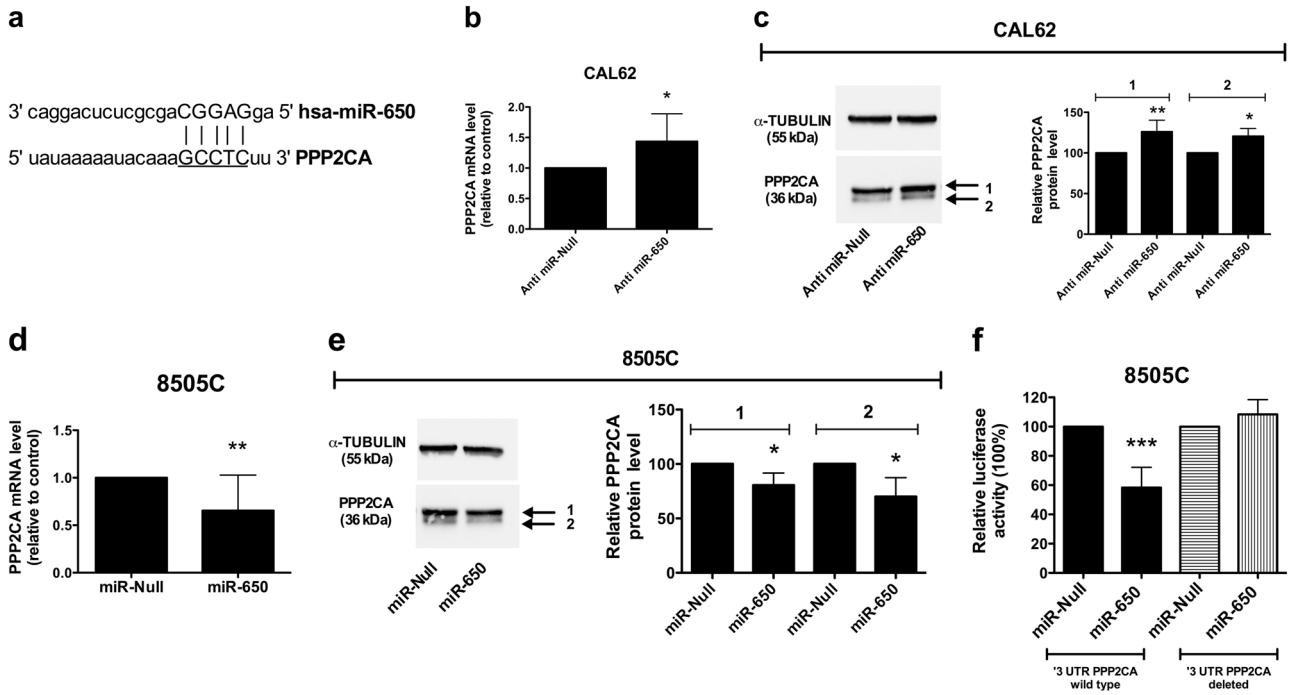

Fig. 6 PPP2CA is a direct target of miR-650. **a** Predicted duplex formation between the human 3′UTR of PPP2CA mRNA and miR-650; the underlined sequence of the 3′UTR of PPP2CA corresponds to the predicted binding site of miR-650 that was deleted (3′UTR deleted). PPP2CA mRNA level was evaluated by q-RT-PCR in CAL62/Anti miR-650 compared to CAL62/Anti miR-Null **b** and in 8505C/miR-650 compared to 8505C/miR-Null cells **d**. Western blots were performed to analyze PPP2CA protein level in CAL62/Anti miR-650 (**c**) and in 8505C miR-650 **e** respect to relative control. Pictures obtained with the Chemidoc (Bio-Rad) are representative of at least three independent experiments. Band intensities of PPP2CA (named 1 and 2) were quantified densitometrically relative to the α TUBULIN (endogenous control); data are reported as average ± SD. **f** Relative luciferase activity was measured in 8505C/miR-650 and in 8505C/miR-Null cells transiently transfected with 3′UTR PPP2CA or with 3′UTR PPP2CA deleted. Luciferase activity was normalized with β-ACTIN plasmid. $*p < 0.05$; $**p < 0.01$; $***p < 0.001$

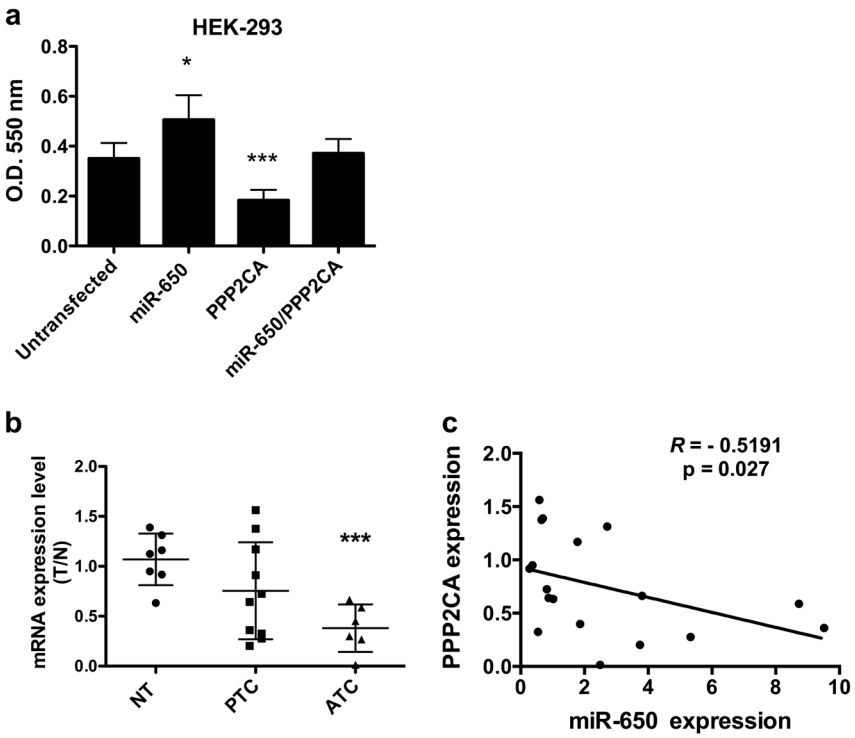

Fig. 7 PPP2CA rescues the phenotype induced by miR-650. **a** HEK-293 cell line was transiently transfected with miR-650, or with PPP2CA, or co-transfected with both plasmids. After 24 h, transfected cells were seeded in the upper chamber of Transwells and migrated cells were quantified at O.D. 550 nm. **b** q-RT-PCR of PPP2CA in NT ($n = 6$), PTC ($n = 10$) and ATC ($n = 5$) snap-frozen tissues. The expression level of PPP2CA was measured by comparing its fluorescence threshold with the average fluorescence threshold of the NT samples. β-ACTIN level was used as an endogenous control. **c** Scatter diagram shows that PPP2CA and miR-650 expression levels are inversely correlated in human thyroid tissues. Spearman's rank correlation test result is reported. $*p < 0.05$; $***p < 0.001$

Through functional experiments, we showed that ectopic expression of miR-650, in 8505C and TPC-1 cells, enhanced cell migration and invasion; while, miR-650 silencing in CAL62 and SW1736 cells induces an opposite phenotype. Thus, in our cell model system, miR-650 acts as an oncomiR.

The different role of miR-650 in different tissues types depends on its target genes. Indeed, in human gastric cancer, high level of miR-650 has been associated with lymphatic and distant metastasis by suppression of the tumor suppressor ING4 [10]. In chronic lymphocytic leukemia, miR-650 is associated with good prognosis and targets proteins important in cell proliferation and survival. Similarly, in colorectal cancer, miR-650 over-expression has a positive association with survival through the inhibition of AKT2/GSK 3β/E-cadherin pathway [25].

Mechanisms of regulation of miRNAs are multiples and can occur at transcriptional and post-transcriptional levels i.e. genetic aberrations, changes in the activity of biogenesis enzyme [26]. The mechanisms modulating miR-650 over-expression in human cancers are poorly known. Recently amplification in band 22q11.2, in the region that encodes miR-650, was found in primary tumor cells isolated from breast cancer patients [8]. Another study showed that miR-650 expression could be induced by p16 (INK4a) [27].

In our thyroid carcinoma model system, miR-650 could be targeted by the multiple genetic lesions responsible of this tumor [14]. A recent paper identified miR-650 among NF-κB deregulated genes in colorectal cancer [28]. Interestingly, NF-κB plays a crucial role in ATC pathogenesis [29]. Finally, miR-650 was found to be up-regulated in our screening of PTC cells (TPC-1) expressing Twist1 transcription factor that are characterized by an aggressive phenotype with increased cell migration and invasion rate [30].

Here, through label-free proteomic screening we unveil a set of novel proteins targets of miR-650. Accordingly to the phenotype induced by miR-650 in our cell model system, we found a deregulation of proteins involved in tight junctions (Supplementary Table 3).

Among deregulated proteins we identified PLAU (Supplementary Table 2, Supplementary Fig. 3a), a protease that degrade the extracellular matrix and that plays an important role in tumor metastasis. Several studies have shown that PLAU is up-regulated in PTC [31].

Here, we focused on up-regulated proteins as we used a cell line in which we stably silenced miR-650. In particular among the 159 up-regulated proteins in CAL62/Anti miR-650 we selected one with the highest score, PPP2CA. We demonstrated that PPP2CA is a target of miR-650 by q-RT-PCR, Western blot and luciferase assay. Strikingly, performing functional experiment in a different human cell line (HEK-293) we showed that restoration of PPP2CA abrogates the motile activity of miR-650. Furthermore, we found a significant inverse correlation between miR-650 and PPP2CA mRNA levels in thyroid tissues.

PP2A is a serine-threonine phosphatase that belongs to a family of proteins that cleaves phosphate from serine and threonine residues of proteins. PP2A is ubiquitously expressed in cells where it regulates various biological process [32, 33]. PP2A can exist in two different forms, as a dimer and as a trimeric form [34]; the dimeric form consists of a structural A and a catalytic C subunit. The trimeric form consists of a structural A, a regulatory B and a catalytic C subunit. PPP2CA encodes the alpha isoform of the catalytic C subunit of PP2A [35].

PP2A has been recently reported to be associated with several types of cancers [36, 37]; in particular its tumor suppressor role has been demonstrated in non-small cell lung [38], prostate [39], breast, gastric [40], renal [41] cancers and leukemia [42].

In agreement, with the effects that we found of miR-650 in thyroid cancer cells, various studies reported that PP2A plays an important role in cell spreading, motility and metastasis [43]. Indeed, it has been shown that PP2A reduce the migration and invasion capability of prostate cancer cells and reduced tumor growth and metastasis in a prostate cancer mouse model [44].

PP2A function can be regulated by structural subunits or by up-regulation of cellular inhibitors such as cell proliferation regulating inhibitor of protein phosphatase 2A (CIP2A). Interestingly, higher CIP2A level occurs in PTC tissues in comparison to adjacent non-tumor tissues [45].

Of note, PP2A is a targetable tumor suppressor [46], this could be achieved through restoration of PP2A [46] by PP2A-activating drugs, or through antagonist of PP2A inhibitors [47–50]. Thus, based on the data obtained here, PP2A could be a novel molecular target in anaplastic thyroid cancer.

Here, we provide the first evidence that miR-650 is an oncomiR in anaplastic thyroid cancers and influence the motile phenotype of thyroid cancer cells. Importantly, our finding implies that the axis miR-650/PPP2CA could be used as biomarker and as a therapeutic target in anaplastic thyroid cancer, for which new therapies are urgently warranted.

Acknowledgements We thank Gennaro Di Maro for its contribution in q-RT-PCR studies.

Funding This study was funded by grants: "Bando di Ateneo per il sostegno alla partecipazione ai bandi di ricerca individuale (quota A per l'anno 2016 e 2017) e ricerca competitiva (quota C per l'anno 2016)" (code DSMB187) from University of Naples "Parthenope" to GS and SO, by 5 × 1000 IRCCS SDN (2013) and by Legge 5/2002 (Annualità 2007) Regione Campania.

Compliance with ethical standards

Conflict of interest The authors declare that they have no conflicts of interest.

Ethical approval All procedures performed in studies involving human participants were in accordance with the ethical standards of the institutional and/or national research committee and with the 1964 Helsinki declaration and its later amendments or comparable ethical standards.

Informed consent Informed consent was obtained from all individual participants included in the study.

Publisher's note: Springer Nature remains neutral with regard to jurisdictional claims in published maps and institutional affiliations.

References

1. D.P. Bartel, MicroRNAs: target recognition and regulatory functions. Cell **136**(2), 215–233 (2009). https://doi.org/10.1016/j.cell.2009.01.002
2. J. Kim, F. Yao, Z. Xiao, Y. Sun, L. Ma, MicroRNAs and metastasis: small RNAs play big roles. Cancer Metas. Rev. (2017). https://doi.org/10.1007/s10555-017-9712-y
3. G.S. Markopoulos, E. Roupakia, M. Tokamani, E. Chavdoula, M. Hatziapostolou, C. Polytarchou, K.B. Marcu, A.G. Papavassiliou, R. Sandaltzopoulos, E. Kolettas, A step-by-step microRNA guide to cancer development and metastasis. Cell Oncol **40**(4), 303–339 (2017). https://doi.org/10.1007/s13402-017-0341-9
4. A.A. Svoronos, D.M. Engelman, F.J. Slack, OncomiR or tumor suppressor? The duplicity of microRNAs in cancer. Cancer Res. **76**(13), 3666–3670 (2016). https://doi.org/10.1158/0008-5472.can-16-0359
5. B. Sun, B. Pu, D. Chu, X. Chu, W. Li, D. Wei, MicroRNA-650 expression in glioma is associated with prognosis of patients. J. Neurooncol. **115**(3), 375–380 (2013). https://doi.org/10.1007/s11060-013-1243-y
6. Z.L. Zeng, F.J. Li, F. Gao, D.S. Sun, L. Yao, Upregulation of miR-650 is correlated with down-regulation of ING4 and progression of hepatocellular carcinoma. J. Surg. Oncol. **107**(2), 105–110 (2013). https://doi.org/10.1002/jso.23210
7. J.Y. Huang, S.Y. Cui, Y.T. Chen, H.Z. Song, G.C. Huang, B. Feng, M. Sun, W. De, R. Wang, L.B. Chen, MicroRNA-650 was a prognostic factor in human lung adenocarcinoma and confers the docetaxel chemoresistance of lung adenocarcinoma cells via regulating Bcl-2/Bax expression. PLoS ONE **8**(8), e72615 (2013). https://doi.org/10.1371/journal.pone.0072615
8. M. Lango-Chavarria, G.K. Chimal-Ramirez, M.E. Ruiz-Tachiquin, N.A. Espinoza-Sanchez, M.C. Suarez-Arriaga, E.M. Fuentes-Panana, A 22q11.2 amplification in the region encoding microRNA-650 correlates with the epithelial to mesenchymal transition in breast cancer primary cultures of Mexican patients. Int. J. Oncol. **50**(2), 432–440 (2017). https://doi.org/10.3892/ijo.2017.3842
9. Z.H. Zuo, Y.P. Yu, Y. Ding, S. Liu, A. Martin, G. Tseng, J.H. Luo, oncogenic activity of miR-650 in prostate cancer is mediated by suppression of CSR1 expression. Am. J. Pathol. **185**(7), 1991–1999 (2015). https://doi.org/10.1016/j.ajpath.2015.03.015
10. X. Zhang, W. Zhu, J. Zhang, S. Huo, L. Zhou, Z. Gu, M. Zhang, MicroRNA-650 targets ING4 to promote gastric cancer tumorigenicity. Biochem. Biophys. Res. Commun. **395**(2), 275–280 (2010). https://doi.org/10.1016/j.bbrc.2010.04.005
11. M. Mraz, D. Dolezalova, K. Plevova, K. Stano Kozubik, V. Mayerova, K. Cerna, K. Musilova, B. Tichy, S. Pavlova, M. Borsky, J. Verner, M. Doubek, Y. Brychtova, M. Trbusek, A. Hampl, J. Mayer, S. Pospisilova, MicroRNA-650 expression is influenced by immunoglobulin gene rearrangement and affects the biology of chronic lymphocytic leukemia. Blood **119**(9), 2110–2113 (2012). https://doi.org/10.1182/blood-2011-11-394874
12. L. Feng, Y. Xie, H. Zhang, Y. Wu, Down-regulation of NDRG2 gene expression in human colorectal cancer involves promoter methylation and microRNA-650. Biochem. Biophys. Res. Commun. **406**(4), 534–538 (2011). https://doi.org/10.1016/j.bbrc.2011.02.081
13. E. Molinaro, C. Romei, A. Biagini, E. Sabini, L. Agate, S. Mazzeo, G. Materazzi, S. Sellari-Franceschini, A. Ribechini, L. Torregrossa, F. Basolo, P. Vitti, R. Elisei, Anaplastic thyroid carcinoma: from clinicopathology to genetics and advanced therapies. Nature reviews. Endocrinology. (2017). https://doi.org/10.1038/nrendo.2017.76
14. J.A. Fagin, S.A. Wells Jr., Biologic and clinical perspectives on thyroid cancer. N. Engl. J. Med. **375**(11), 1054–1067 (2016). https://doi.org/10.1056/NEJMra1501993
15. M. Boufraqech, J. Klubo-Gwiezdzinska, E. Kebebew, MicroRNAs in the thyroid. Best practice & research. Clin. Endocrinol. Metab. **30**(5), 603–619 (2016). https://doi.org/10.1016/j.beem.2016.10.001
16. M. Saiselet, J.M. Pita, A. Augenlicht, G. Dom, M. Tarabichi, D. Fimereli, J.E. Dumont, V. Detours, C. Maenhaut, miRNA expression and function in thyroid carcinomas: a comparative and critical analysis and a model for other cancers. Oncotarget **7**(32), 52475–52492 (2016). https://doi.org/10.18632/oncotarget.9655
17. C.S. Fuziwara, E.T. Kimura, MicroRNAs in thyroid development, function and tumorigenesis. Mol. Cell. Endocrinol. **456**, 44–50 (2017). https://doi.org/10.1016/j.mce.2016.12.017
18. E. Imperlini, I. Colavita, M. Caterino, P. Mirabelli, D. Pagnozzi, L. Del Vecchio, R. Di Noto, M. Ruoppolo, S. Orru, The secretome signature of colon cancer cell lines. J. Cell. Biochem. **114**(11), 2577–2587 (2013). https://doi.org/10.1002/jcb.24600
19. E. Nigro, E. Imperlini, O. Scudiero, M.L. Monaco, R. Polito, G. Mazzarella, S. Orru, A. Bianco, A. Daniele, Differentially expressed and activated proteins associated with non small cell lung cancer tissues. Respir. Res. **16**, 74 (2015). https://doi.org/10.1186/s12931-015-0234-2
20. M. Caterino, C. Corbo, E. Imperlini, M. Armiraglio, E. Pavesi, A. Aspesi, F. Loreni, I. Dianzani, M. Ruoppolo, Differential proteomic analysis in human cells subjected to ribosomal stress. Proteomics. **13**(7), 1220–1227 (2013). https://doi.org/10.1002/pmic.201200242
21. S. Spaziani, E. Imperlini, A. Mancini, M. Caterino, P. Buono, S. Orru, Insulin-like growth factor 1 receptor signaling induced by supraphysiological doses of IGF-1 in human peripheral blood lymphocytes. Proteomics. **14**(13-14), 1623–1629 (2014). https://doi.org/10.1002/pmic.201300318
22. M. Caterino, A. Pastore, M.G. Strozziero, G. Di Giovamberardino, E. Imperlini, E. Scolamiero, L. Ingenito, S. Boenzi, F. Ceravolo, D. Martinelli, C. Dionisi-Vici, M. Ruoppolo, The proteome of cblC defect: in vivo elucidation of altered cellular pathways in humans. J. Inherit. Metab. Dis. **38**(5), 969–979 (2015). https://doi.org/10.1007/s10545-014-9806-4
23. E. Minna, P. Romeo, M. Dugo, L. De Cecco, K. Todoerti, S. Pilotti, F. Perrone, E. Seregni, L. Agnelli, A. Neri, A. Greco, M.G. Borrello, miR-451a is underexpressed and targets AKT/mTOR pathway in papillary thyroid carcinoma. Oncotarget **7**(11), 12731–12747 (2016). https://doi.org/10.18632/oncotarget.7262
24. A.A. Farooqi, M.Z. Qureshi, E. Coskunpinar, S.K. Naqvi, I. Yaylim, M. Ismail, MiR-421, miR-155 and miR-650: emerging

trends of regulation of cancer and apoptosis. Asian Pacific J Cancer Prevent **15**(5), 1909–1912 (2014)
25. C. Zhou, F. Cui, J. Li, D. Wang, Y. Wei, Y. Wu, J. Wang, H. Zhu, S. Wang, MiR-650 represses high-risk non-metastatic colorectal cancer progression via inhibition of AKT2/GSK3beta/E-cadherin pathway. Oncotarget **8**(30), 49534–49547 (2017). https://doi.org/10.18632/oncotarget.17743
26. L.A. Yates, C.J. Norbury, R.J. Gilbert, The long and short of microRNA. Cell **153**(3), 516–519 (2013). https://doi.org/10.1016/j.cell.2013.04.003
27. W.W. Chien, C. Domenech, R. Catallo, T. Kaddar, J.P. Magaud, G. Salles, M. Ffrench, Cyclin-dependent kinase 1 expression is inhibited by p16(INK4a) at the post-transcriptional level through the microRNA pathway. Oncogene **30**(16), 1880–1891 (2011). https://doi.org/10.1038/onc.2010.570
28. M.L. Slattery, L.E. Mullany, L. Sakoda, W.S. Samowitz, R.K. Wolff, J.R. Stevens, J.S. Herrick, The NF-kappaB signalling pathway in colorectal cancer: associations between dysregulated gene and miRNA expression. J. Cancer Res. Clin. Oncol. (2017). https://doi.org/10.1007/s00432-017-2548-6
29. F. Pacifico, A. Leonardi, Role of NF-kappaB in thyroid cancer. Mol. Cell. Endocrinol. **321**(1), 29–35 (2010). https://doi.org/10.1016/j.mce.2009.10.010
30. F.M. Orlandella, G. Di Maro, C. Ugolini, F. Basolo, G. Salvatore, TWIST1/miR-584/TUSC2 pathway induces resistance to apoptosis in thyroid cancer cells. Oncotarget **7**(43), 70575–70588 (2016). https://doi.org/10.18632/oncotarget.12129
31. J. Qiu, W. Zhang, Q. Xia, F. Liu, L. Li, S. Zhao, X. Gao, C. Zang, R. Ge, Y. Sun, RNA sequencing identifies crucial genes in papillary thyroid carcinoma (PTC) progression. Exp. Mol. Pathol. **100**(1), 151–159 (2016). https://doi.org/10.1016/j.yexmp.2015.12.011
32. A.A. Sablina, W.C. Hahn, The role of PP2A A subunits in tumor suppression. Cell Adhes. Migr. **1**(3), 140–141 (2007)
33. A. Bononi, C. Agnoletto, E. De Marchi, S. Marchi, S. Patergnani, M. Bonora, C. Giorgi, S. Missiroli, F. Poletti, A. Rimessi, P. Pinton, Protein kinases and phosphatases in the control of cell fate. Enzyme Res. **2011**, 329098 (2011). https://doi.org/10.4061/2011/329098
34. V. Janssens, J. Goris, Protein phosphatase 2A: a highly regulated family of serine/threonine phosphatases implicated in cell growth and signalling. Biochem. J. **353**(Pt 3), 417–439 (2001)
35. S. Longin, K. Zwaenepoel, J.V. Louis, S. Dilworth, J. Goris, V. Janssens, Selection of protein phosphatase 2A regulatory subunits is mediated by the C terminus of the catalytic Subunit. J. Biol. Chem. **282**(37), 26971–26980 (2007). https://doi.org/10.1074/jbc.M704059200
36. J. Westermarck, W.C. Hahn, Multiple pathways regulated by the tumor suppressor PP2A in transformation. Trends Mol. Med. **14**(4), 152–160 (2008). https://doi.org/10.1016/j.molmed.2008.02.001
37. R. Zimmerman, D.J. Peng, H. Lanz, Y.H. Zhang, A. Danen-Van Oorschot, S. Qu, C. Backendorf, M. Noteborn, PP2A inactivation is a crucial step in triggering apoptin-induced tumor-selective cell killing. Cell Death Dis. **3**, e291 (2012). https://doi.org/10.1038/cddis.2012.31
38. X. Tan, M. Chen, MYLK and MYL9 expression in non-small cell lung cancer identified by bioinformatics analysis of public expression data. Tumour Biol. **35**(12), 12189–12200 (2014). https://doi.org/10.1007/s13277-014-2527-3
39. A.P. Singh, S. Bafna, K. Chaudhary, G. Venkatraman, L. Smith, J. D. Eudy, S.L. Johansson, M.F. Lin, S.K. Batra, Genome-wide expression profiling reveals transcriptomic variation and perturbed gene networks in androgen-dependent and androgen-independent prostate cancer cells. Cancer Lett. **259**(1), 28–38 (2008). https://doi.org/10.1016/j.canlet.2007.09.018
40. T. Huang, K. He, Y. Mao, M. Zhu, C. Yan, F. Yu, Q. Qi, T. Wang, Y. Wang, J. Du, L. Liu, Genetic variants in PPP2CA are associated with gastric cancer risk in a Chinese population. Sci. Rep. **7**(1), 11499 (2017). https://doi.org/10.1038/s41598-017-12040-z
41. J. Li, C. Sheng, W. Li, J.H. Zheng, Protein phosphatase-2A is down-regulated in patients within clear cell renal cell carcinoma. Int. J. Clin. Exp. Pathol. **7**(3), 1147–1153 (2014)
42. E. Arriazu, R. Pippa, M.D. Odero, Protein phosphatase 2A as a therapeutic target in acute myeloid leukemia. Front. Oncol. **6**, 78 (2016). https://doi.org/10.3389/fonc.2016.00078
43. S. Basu, PP2A in the regulation of cell motility and invasion. Current Protein Pept Sci **12**(1), 3–11 (2011)
44. A. Bhardwaj, S. Singh, S.K. Srivastava, S. Arora, S.J. Hyde, J. Andrews, W.E. Grizzle, A.P. Singh, Restoration of PPP2CA expression reverses epithelial-to-mesenchymal transition and suppresses prostate tumour growth and metastasis in an orthotopic mouse model. Br. J. Cancer **110**(8), 2000–2010 (2014). https://doi.org/10.1038/bjc.2014.141
45. T.T. Chao, H.C. Maa, C.Y. Wang, D. Pei, Y.J. Liang, Y.F. Yang, S.J. Chou, Y.L. Chen, CIP2A is a poor prognostic factor and can be a diagnostic marker in papillary thyroid carcinoma. APMIS **124**(12), 1031–1037 (2016). https://doi.org/10.1111/apm.12602
46. C.M. O'Connor, A. Perl, D. Leonard, J. Sangodkar, G. Narla, Therapeutic Targeting of PP2A. Int. J. Biochem. Cell Biol. (2017). https://doi.org/10.1016/j.biocel.2017.10.008
47. P.P. Ruvolo, The broken "Off" switch in cancer signaling: PP2A as a regulator of tumorigenesis, drug resistance, and immune surveillance. BBA Clin. **6**, 87–99 (2016). https://doi.org/10.1016/j.bbacli.2016.08.002
48. I. Cristobal, L. Garcia-Orti, C. Cirauqui, X. Cortes-Lavaud, M.A. Garcia-Sanchez, M.J. Calasanz, M.D. Odero, Overexpression of SET is a recurrent event associated with poor outcome and contributes to protein phosphatase 2A inhibition in acute myeloid leukemia. Haematologica **97**(4), 543–550 (2012). https://doi.org/10.3324/haematol.2011.050542
49. I. Cristobal, L. Garcia-Orti, C. Cirauqui, M.M. Alonso, M.J. Calasanz, M.D. Odero, PP2A impaired activity is a common event in acute myeloid leukemia and its activation by forskolin has a potent anti-leukemic effect. Leukemia **25**(4), 606–614 (2011). https://doi.org/10.1038/leu.2010.294
50. D. Perrotti, P. Neviani, Protein phosphatase 2A: a target for anticancer therapy. Lancet. Oncol. **14**(6), e229–e238 (2013). https://doi.org/10.1016/s1470-2045(12)70558-2